

EXPERIMENTAL TESTS OF INTERNAL COMPOSITE STEEL FRAMES AGAINST PROGRESSIVE COLLAPSE

B. YANG¹ and K. H. TAN²

ABSTRACT

In this paper, four internal composite steel frames are tested under a middle-column-removal scenario. Two types of connections, including web cleat and flush end plate, are studied. In addition, the effect of reinforcement ratio has been investigated. The contributions from two types of mechanisms, namely, flexural action and catenary action, have been identified. The experimental results demonstrate that catenary action can be formed in the internal composite frames. Beam-column joint failure always controls the ultimate resistances of the internal composite frames. It is also found that higher flexural action and catenary action were observed if additional reinforcement bars are provided in composite slabs.

Introduction

After the partial collapse of the Ronan Point apartment tower in 1968, researchers and engineers began to realise the importance of structural resistance to progressive collapse. More and more research works and design efforts are directed to this area, especially after the World Trade Centre disaster on 11 September 2001. The alternate load path method, an important design approach to mitigate progressive collapse, has been included by a number of design codes including GSA (2003) and DoD (2009). This approach allows local failure to occur when subjected to an extreme load, but seeks to provide alternate load paths so that the initial damage can be contained and major collapse can be averted.

In the alternate load path method, the middle joint above the removed column shown in Figure 1, is subjected to a sagging moment while the side joints are under hogging moments. Due to the presence of composite slabs above steel joints, the structural behaviour of side and middle composite joints, including flexural and catenary resistances and rotation capacities, is different with each other. Yang and Tan (2012) presents a series of experimental tests of composite beam-column joints under a middle-column-removal scenario. It consisted of two types of tests, namely, middle joints under sagging moment and side joints under hogging moment. For the middle and side joints, it was observed from the experimental results that the obtained load-displacement curves were quite different. At flexural action stage, the load-carrying capacities of the side joints were much greater than the middle joints. In this series of tests, an inflection point was assumed to be located at the middle of the beam span. However, during the deflection process, the inflection point may change its location due to the load resistance difference of middle and side joints. The interaction between the middle and the side joints will be studied in this paper by experimental tests. The load redistribution after the column removal will be addressed.

¹Ph. D. Student, School of Civil & Environmental Engineering, Nanyang Technological University, 50 Nanyang Avenue, Singapore, 639798

²Professor, School of Civil & Environmental Engineering, Nanyang Technological University, 50 Nanyang Avenue, Singapore, 639798

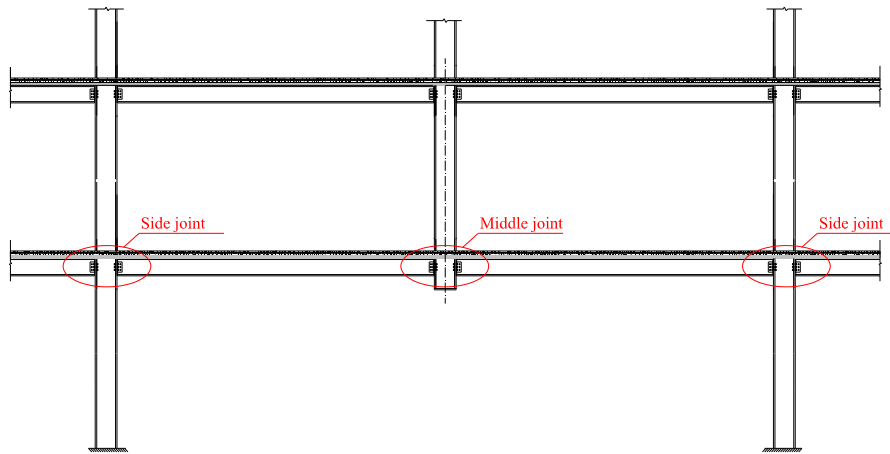


Figure 1. Composite frame subjected to a middle-column-removal scenario

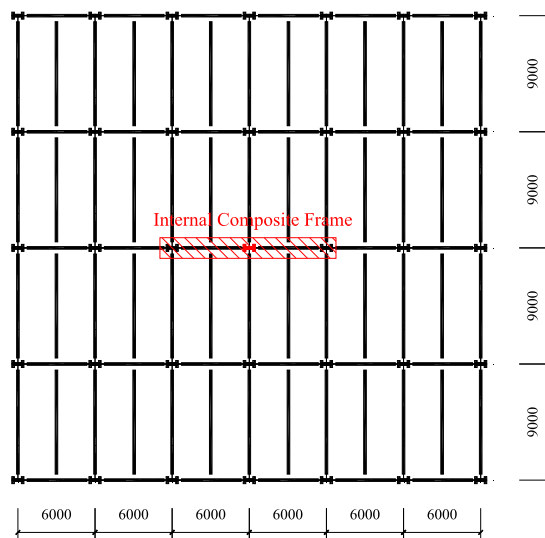


Figure 2. Plan view of the prototype internal composite structure

Test Set-up and Specimens

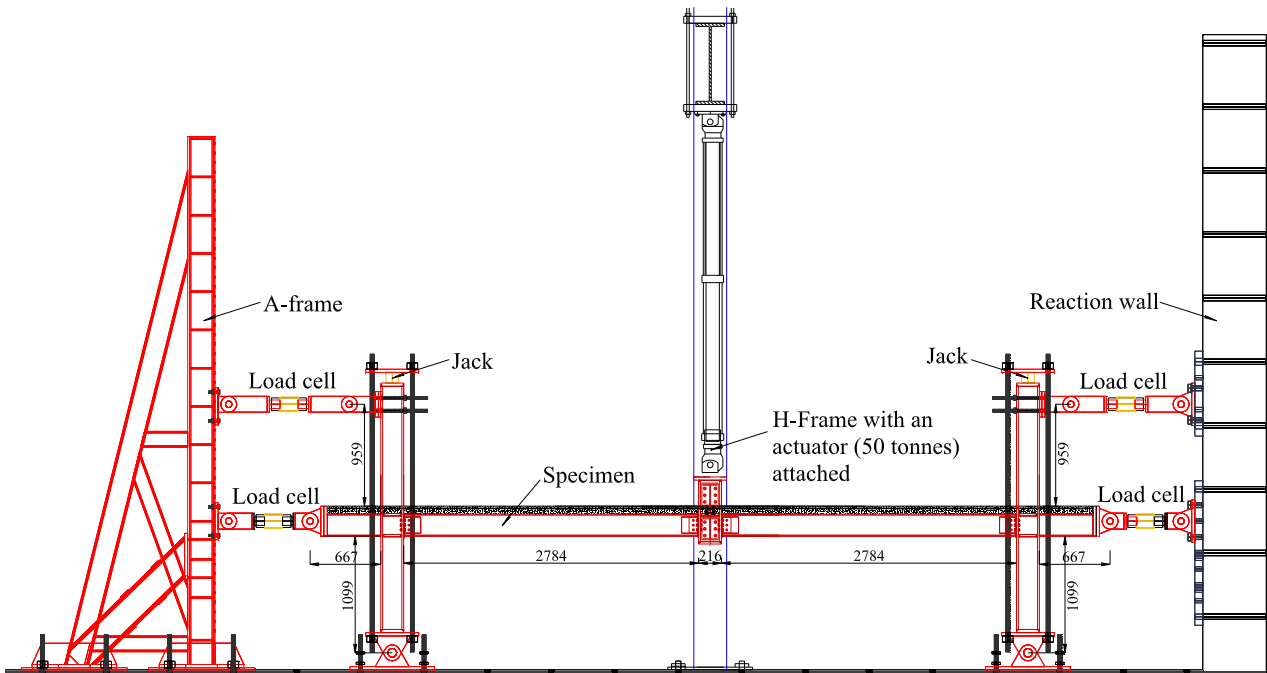
Test set-up

The plan view of the prototype composite structure is shown in Figure 2. As shown in Figure 2, the considered Internal Composite Frames represents full horizontal restraints, which are provided by the surrounding structural elements. The vertical loads are applied under in-plane loading condition. Due to space limitation in the laboratory, the test specimens were scaled down to 1/2 of their original size.

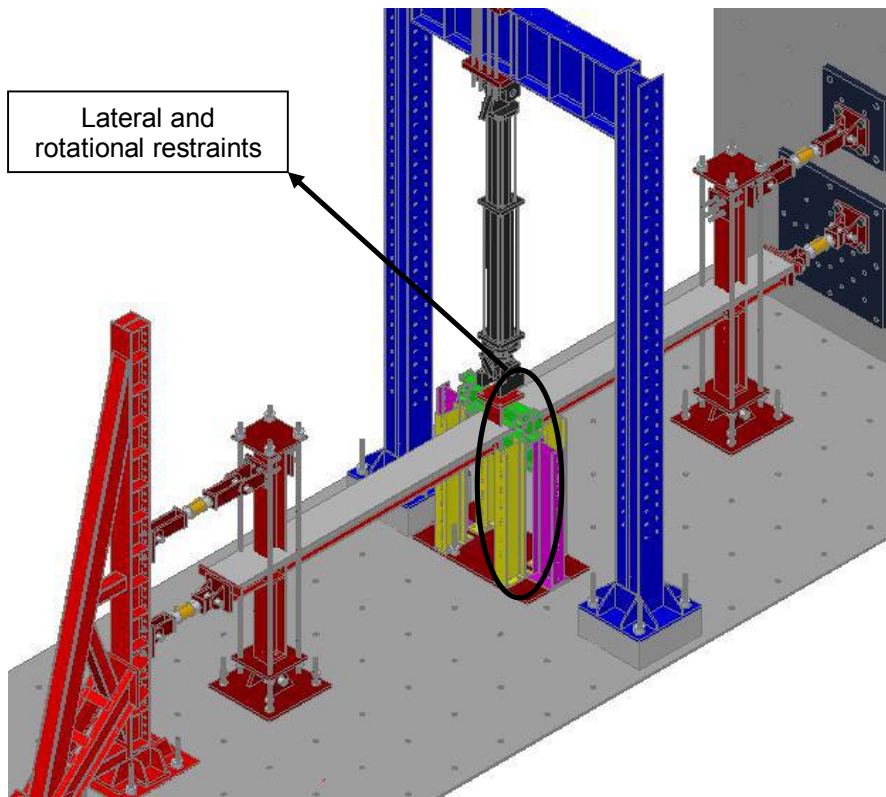
Figures 3 (a) and (b) show the test set-up for the frame specimens. The top and bottom ends of the two columns were connected to the pin supports, which represent the restraints of the surrounding structural elements. In addition, the extended beams were also horizontally restrained by two pin-pin connections. As shown in Figure 3, the horizontal restraints in this test set-up are provided by an A-frame and a reaction wall. Four load cells have been used in order to measure the horizontal reaction forces. The horizontal reactions at the column bottom ends are obtained by the bending moments of the steel column sections, which are measured by strain gauges.

To consider the effect of column axial forces on the behaviour of the internal composite steel frames, hydraulic jacks were installed at the tops of the two columns to apply constant axial loads onto the columns. In order to consider the rotational restraint to beam-column joints from the continuous column of upper storeys, the test rig included a rotational restraint system at the mid-span, as shown in Figure 4. The column rotation was restrained by sixteen steel rollers (Roller 2 shown in Figure 4), which would bear against the flanges of four steel columns during testing. In addition, the beam-column joints were restrained from lateral

movement by a lateral restraint system (Roller 1 shown in Figure 4). A displacement-controlled point load was applied to the middle column using an actuator, which was reacted against a strong H-frame. Load was applied under displacement control at a rate of 6 mm/min. A pair of secondary loading beams shown in Figure 4, was also connected to the middle column, to ensure the line load could be applied onto the composite slabs directly.



(a) Front view



(b) Aerial view

Figure 3. Test set-up (unit: mm)

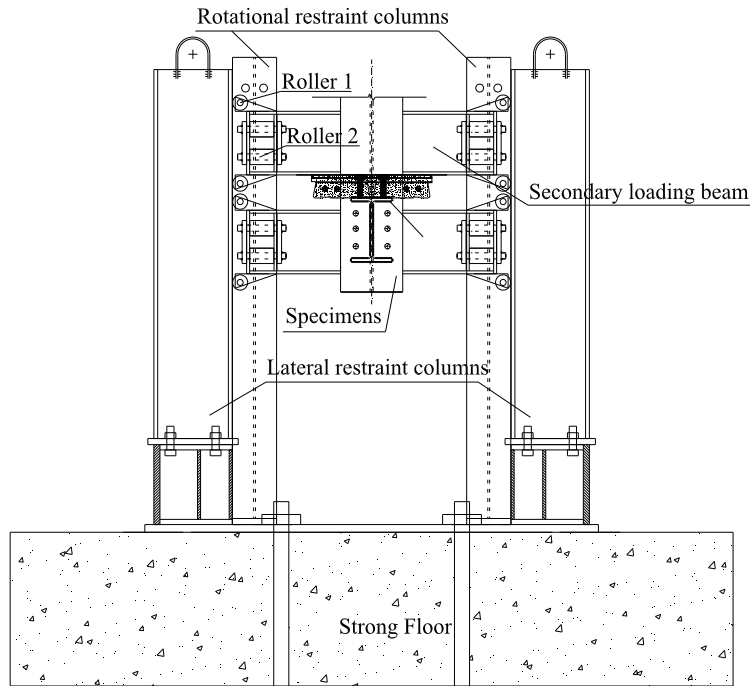


Figure 4. Lateral and rotational restraint systems

Test specimens

All specimens had the same total length of 7,290 mm. The configurations of the specimens are illustrated in Figure 5. In this experimental programme, two types of connections including web cleat and flush end plate connections, were tested. All the connection details of these two types of connections are shown in Figure 6. Two types of reinforcement details have been tested in this series of experimental programme. One type of reinforcement details is steel mesh with 4T13 bars and the other type of reinforcement details is steel mesh only. The beam and column cross-sections of all the specimens were the same, viz. UB254×146×37 and UC203×203×71. The beams and columns were strengthened by some stiffeners or welded thick plates to limit the influence of beam and column deformations on the connection behaviour. As shown in Figure 6, two rows of shear studs with a displacement of 90mm were welded along the steel beams in order to ensure the full shear connection between steel beam and composite slab. The details of the four composite joint specimens are also presented in Table 1. The reference used for the specimens follows the nomenclature *I-W(F)-MT(M)* where *I* represents internal composite frames, *W* represents web cleat connection, *F* represents flush end plate connection, *MT* represents the reinforcement of steel mesh and 4T13 bars and *M* represents the reinforcement of steel mesh. For instance, in *I-W-MT*, the specimen represents the *internal composite steel frame*, the connection type is *web cleat* and the composite slab reinforcement is *steel mesh and 4T13 bars*.

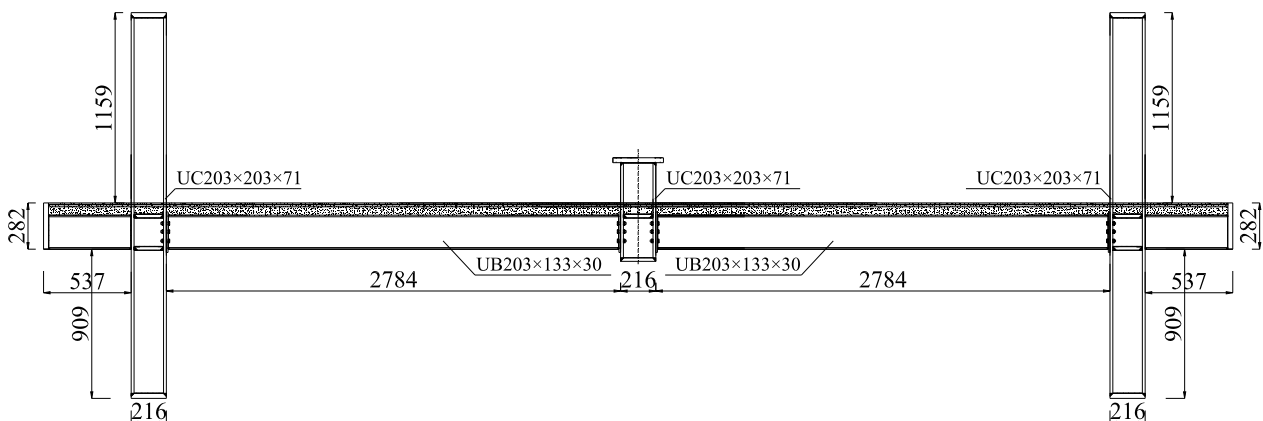


Figure 5. Layout of the internal composite steel frame specimens

Table 1. Summary of composite steel frame specimens

Specimen ID	Connection type	Bolt	End plate/angle	Reinforcement
I-W-MT	Web cleat	Grade 8.8 M20	L90×9	Steel mesh and 4T13
I-F-MT	Flush end plate	Grade 8.8 M16	200×10	Steel mesh and 4T13
I-W-M	Web cleat	Grade 8.8 M20	L90×9	Steel mesh
I-F-M	Flush end plate	Grade 8.8 M16	200×10	Steel mesh

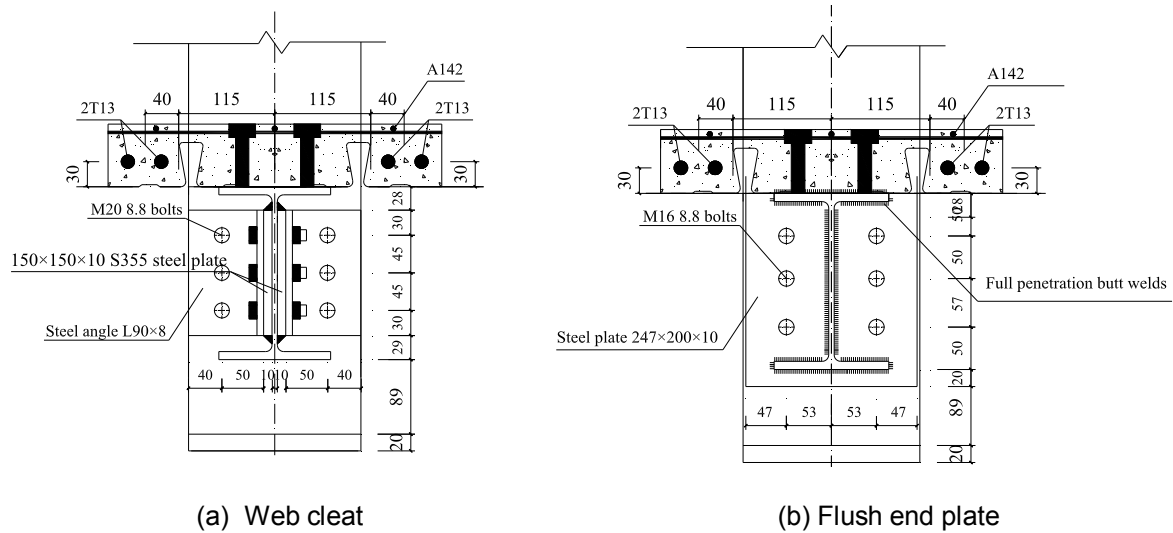


Figure 6. Beam-column joint details of the internal composite steel frame specimens

Material properties

Material tests were conducted to obtain the representative stress-strain curves for analysis purpose. These include tensile testing of steel angles, flush end plate, steel profile decking, steel beams and reinforcement, and compressive and tensile tests of concrete.

The tensile test results of structural steel including steel angles, 10 mm thick flush end plate, profile decking, beam flange and web, column flange and web, T13 reinforcement and R6 reinforcement, are presented in Table 2. Grade 8.8 bolts were used for all specimens. A grade 8.8 bolt has a nominal ultimate tensile strength of 800MPa and a nominal yield strength of 640MPa. Both compressive test and indirect splitting test were conducted to obtain the compressive and tensile strength of concrete. The average concrete compressive and tensile strengths were 25.95MPa and 2.18MPa, respectively.

Table 2 Tensile test results of structural steel from composite joint test specimens

Coupon plate	Yield strength (MPa)	Ultimate strength (MPa)	Ultimate strain*
L 90×8 angle	316	446	0.310
10 mm thick end plate	295	427	0.332
Profile decking	647	667	0.12
Beam flange	434	537	0.26
Beam web	458	546	0.286
Column flange	403	544	0.275
Column web	416	553	0.264
T13 reinforcement	615	705	0.124
R6 reinforcement	450	527	0.249

Experimental Results

In this section, the experimental results of four composite steel frames are presented. A summary of the test results is found in Table 3, from which the maximum vertical loads, the corresponding middle column displacement and rotation angles are given. The axial forces of beams are also included in this table. Figure 7 shows the overall deformations of the frame specimens. From these two figures it can be found that the displacement profile of each beam can be approximated by a straight line, which indicates the formation of plastic hinges at the beam-column connections. It should be mentioned that at Table 3 the joint rotation angles at maximum loads are obtained by dividing the centre column displacement at the maximum load by the beam span of 2.784m, as shown in Figure 3 (a). This simplification is reasonable because the beam deflection profiles between the plastic hinges can be approximated by straight lines.

Table 3 List of test results

Specimen ID	I-W-MT	I-F-MT	I-W-M	I-F-M
Maximum vertical load (kN)	274	253	150	148
Displacement at maximum load (mm)	640	576	637	566
Joint rotation at maximum load (degree)	12.95	11.69	12.89	11.49
Maximum axial fore of the beam (kN)	673	700	385	436



(a) Deformation of specimens with 4T13 rebars



(b) Deformation of specimens without 4T13 rebars

Figure 7. Overall deformation of composite steel frame specimens

Specimen I-W-MT

Figure 8 shows the vertical force-middle column displacement relationship for Specimen I-W-MT. It can be seen that at the initial loading stage, the applied load was resisted by flexural action while at large deformation stage, the load was resisted by catenary action. Figure 8 shows that catenary action could not be mobilized until the vertical displacement of the middle column was greater than 300mm. The failure mode of this specimen is shown in Figure 9. At a displacement of 96mm, a longitudinal crack formed in the composite slab, which has been shown in Figure 7 (a). The longitudinal crack indicates the bond-slip failure of T13 reinforcing bars in the composite slab. However, the bond-slip failure does not mean the failure of reinforcing bars. T13 bars could still resist the applied load like cables. Concrete crushed severely in compression during testing at the middle beam-column joint, as shown in Figure 9. One of the web angles fractured at a displacement of 640mm, which caused a significant reduction of applied load. Finally, one of the T13 reinforcing bars at the left side beam-column joint fractured at a displacement of 652mm, which has also been shown in Figure 9.

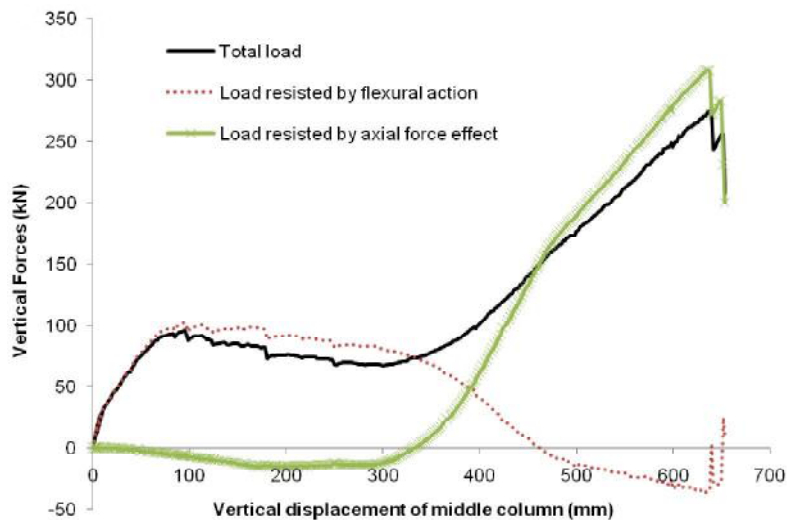


Figure 8. Vertical force-middle column displacement curve of Specimen I-W-MT



Figure 9. Failure mode of Specimen I-W-MT

Specimen I-F-MT

Figure 10 shows the force-displacement history of Specimen I-F-MT. Similar with Specimen I-W-MT, the force-displacement history can be divided into two stages: flexural action and catenary action. Figure 11 shows the failure mode of this specimen. At a displacement of 460mm, one of the bolts at the middle beam-column joint fractured. Final failure was controlled by bolt fracture at the right beam-column joints, which has been shown in Figure 11.

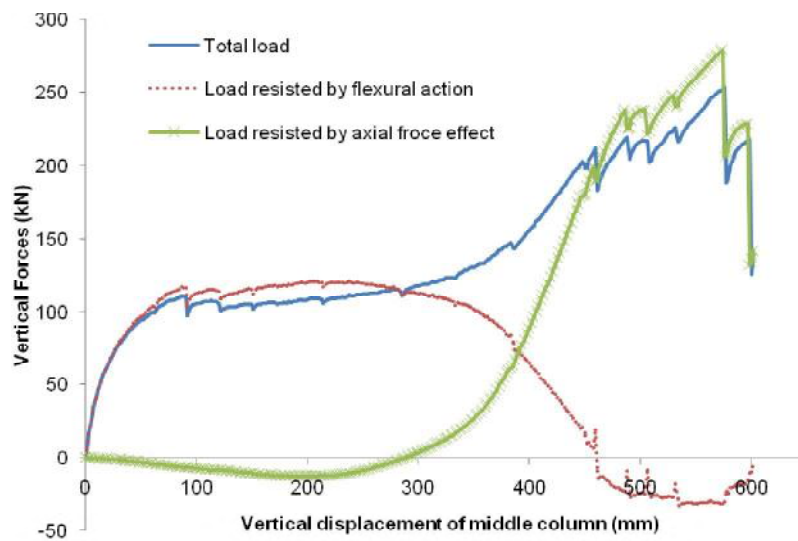


Figure 10. Vertical force-middle column displacement curve of Specimen I-F-MT



Figure 11. Failure mode of Specimen I-F-MT

Specimen I-W-M

Figure 12 compares the force-displacement curve of Specimen I-W-MT with Specimen I-W-M, which shows the effect of 4T13 reinforcing bars clearly. It can be found from this figure that 4T13 bars can increase the load-carrying resistance not only at flexural action stage but also at catenary action stage significantly. Figure 13 shows the failure mode of this specimen. The final failure is controlled by bolted angle fracture, which is the same with Specimen I-W-MT. At large deformation stage, after the fracture of profile decking and steel mesh, the composite slab was broken completely at side beam-column joints, as shown in Figure 13. It means only steel connection (bolted angle connections) resisted the applied loads.

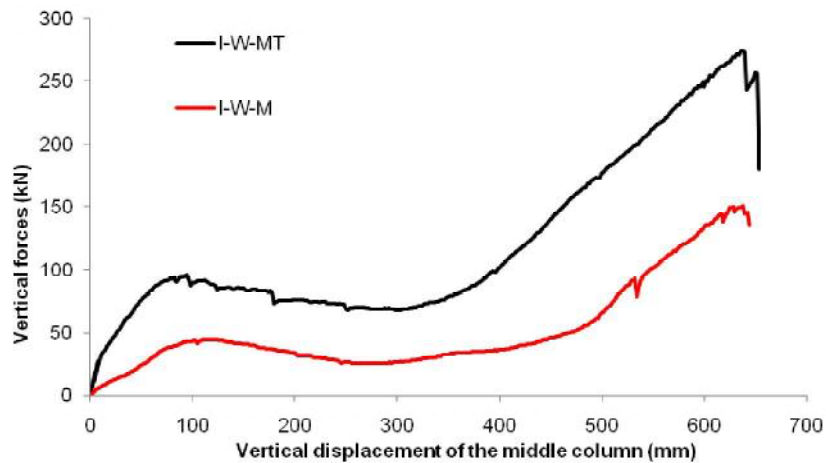


Figure 12. Vertical force-middle column displacement curves of Specimens I-W-MT and I-W-M



Figure 13. Failure mode of Specimen I-W-M

Specimen I-F-M

Figure 14 compares the force-displacement curve of Specimen I-F-MT with Specimen I-F-M. It can be found from this figure that for this type of connection (flush end plate connections), 4T13 bars can also increase the load-carrying resistance at flexural action stage and at catenary action stage. It should also be mentioned that the contribution of 4T13 bars for flush end plate connections is not as significant as web cleat connections, especially at flexural action stage. This is because flush end plate connection belongs to semi-

rigid connections, which have higher flexural resistances than simple connections like web cleat connections. Therefore, the increase of load-carrying capacity caused by 4T13 reinforcing bars is relatively lower than web cleat connections. Figure 15 shows the failure mode of this specimen. The final failure is controlled by bolt fracture, which is the same with Specimen I-F-MT. To be similar with Specimen I-W-M, at large deformation stage, after the fracture of profile decking and steel mesh, the composite slab was broken completely at side beam-column joints, as shown in Figure 15, and only steel connection (flush end plate connections) resisted the applied loads.

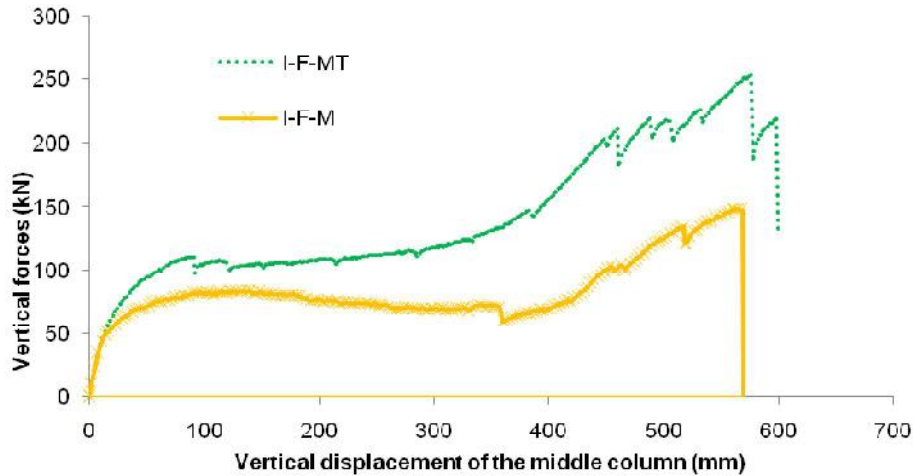


Figure 14. Vertical force-middle column displacement curves of Specimens I-F-MT and I-F-M



Figure 15. Failure mode of Specimen I-F-M

Conclusions

In this study, four experimental tests were conducted to investigate the behaviour of internal composite steel frames under a middle-column-removal scenario. Composite web cleat and flush end plate connections were studied. The contributions from two types of mechanisms, namely, flexural action and catenary action, have been identified. The experimental results demonstrate that catenary action can be formed in the internal composite frames. Beam-column joint failure always controls the ultimate resistances of the internal composite frames. It is also found that higher flexural action and catenary action were observed if additional reinforcement bars are provided in composite slabs.

References

- Yang, B., and K. H. Tan, 2012. Behaviour of composite beam-column joints under a middle-column-removal scenario: experimental tests. *Journal of Structural Engineering-ASCE* (submitted for publication).
- Department of Defense (DOD), 2009. *Design of Buildings to Resist Progressive Collapse*, Unified Facilities Criteria, 4-023-03, USA.
- General Services Administration (GSA), 2003. *Progressive Collapse Analysis and Design Guidelines for New Federal Office Buildings and Major Modernization Projects*, Washington, D.C., USA.